

Mechanism of robust circadian oscillation of KaiC phosphorylation *in vitro*

Kohei Eguchi^{*}, Mitsumasa Yoda^{*}, Tomoki P. Terada, and Masaki Sasai

Department of Computational Science and Engineering, Nagoya University, Nagoya
464-8603, Japan

ABSTRACT

By incubating the mixture of three cyanobacterial proteins, KaiA, KaiB, and KaiC, with ATP *in vitro*, Kondo and his colleagues reconstituted the robust circadian rhythm of the phosphorylation level of KaiC (*Science*, 308; 414-415 (2005)). This finding indicates that protein-protein interactions and the associated hydrolysis of ATP suffice to generate the circadian rhythm. Several theoretical models have been proposed to explain the rhythm generated in this “protein-only” system, but the clear criterion to discern different possible mechanisms was not known. In this paper, we discuss a model based on the two basic assumptions: The assumption of the allosteric transition of a KaiC hexamer and the assumption of the monomer exchange between KaiC hexamers. The model shows a stable rhythmic oscillation of the phosphorylation level of KaiC, which is robust against changes in concentration of Kai proteins. We show that this robustness gives a clue to distinguish different possible mechanisms. We also discuss the robustness of oscillation against the change in the system size. Behaviors of the system with the cellular or subcellular size should shed light on the role of the protein-protein interactions in *in vivo* circadian oscillation.

^{*}These two authors equally contributed to this work.

INTRODUCTION

To resolve the mechanism of circadian rhythms, cyanobacteria have been studied as the simplest organisms to exhibit rhythms. In a cyanobacterium *Synechococcus elongatus* PCC 7942, the gene cluster *kaiABC* and their product proteins, KaiA, KaiB, and KaiC, were shown to be essential in generating the rhythm (1), and intense interest has been focused on these Kai proteins (2-19). In the recent study of Kondo and his colleague (20), the circadian oscillation in the phosphorylation level of KaiC has been reconstituted *in vitro* by incubating the mixture of KaiA, KaiB, and KaiC with ATP. This epoch-making work indicates that protein-protein interactions (21) and the associated hydrolysis of ATP (22) suffice to generate the rhythm in the absence of transcriptional or translational processes.

Interactions between Kai proteins *in vitro* have been characterized in detail (4, 19, 21, 23-26): KaiC has the autophosphatase activity, so that KaiC is gradually dephosphorylated when KaiC alone is incubated *in vitro* (19). KaiC is phosphorylated when KaiC is incubated with KaiA (4, 19, 21), whereas KaiB attenuates the activity of KaiA (4, 21). These observations suggest the scenario that KaiC with the low phosphorylation level interacts with KaiA to make the phosphorylation level high, which then allows interaction between KaiC and KaiB to make the phosphorylation level low. The mixture solution of KaiA, KaiB, and KaiC, therefore should have two phases, the phase of phosphorylation with lower affinity of KaiC to KaiB and the phase of dephosphorylation with higher affinity of KaiC to KaiB. Such phosphorylation dependent interactions among Kai proteins (21, 23) and existence of the two phases (23) were confirmed by experiments. However, the precise mechanism of the robust oscillations remains unclear, which calls for *in silico* modeling of the biochemical network of Kai proteins.

Although the two phases of phosphorylation and dephosphorylation are discernible experimentally, the difference of the system in these two phases is unknown. As KaiC forms hexamer in solution (7, 8, 21), van Zon *et al.* (27) and Yoda *et al.* (28) have assumed that a KaiC hexamer switches between two different structural states in the two phases, each of which has the different affinity to KaiA or KaiB. Figure 1 is the simplest reaction scheme based on this assumption of the allosteric transition of the KaiC hexamer. In this reaction scheme, it is obvious that each individual KaiC hexamer switches between the two phases and therefore shows oscillation in its phosphorylation level. However, because the reactions occur stochastically at different timings, the phosphorylation level of independent KaiC hexamers should be desynchronized, even if all the KaiC hexamers are in the same oscillatory phase at the beginning. Such

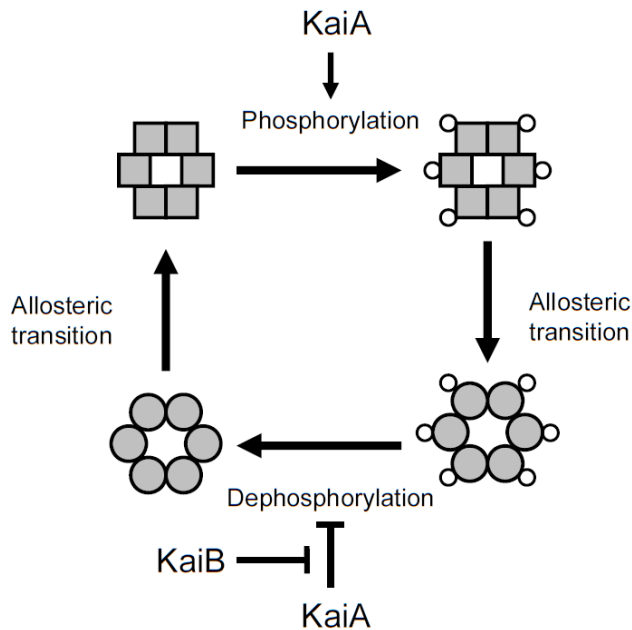


Figure 1

The simplest reaction scheme assuming only the allosteric transition of the KaiC hexamer. The KaiC hexamer undergoes the allosteric transition from one structural state to the other when the phosphorylation level of KaiC is high, and the reverse transition is induced when the phosphorylation level is low. In one structural state, KaiC is phosphorylated by the kinase reaction of KaiA. In the other structural state, KaiC has the higher binding affinity to KaiB, so that KaiB inhibits KaiA from catalyzing phosphorylation. In the latter case, KaiC is dephosphorylated by the autophosphatase reaction of KaiC.

desynchronization should smear out the oscillation in the phosphorylation level of the ensemble of KaiC hexamers, but the observed clear and robust oscillation of the phosphorylation level of the ensemble of many KaiC hexamers strongly suggests that there exists some communication among KaiC hexamers, which synchronizes the phosphorylation level of many KaiC hexamers.

The simplest explanation of this communication would be the complex formation among KaiC hexamers to promote or to suppress phosphorylation or dephosphorylation (29-31). Such interactions should constitute the nonlinear feedback loop, which can stabilize the synchronized oscillation of the phosphorylation level of many of KaiC hexamers. There is, however, no experimental data to support existence of such direct interactions among KaiC hexamers, and hence in this paper, we do not pursue this line.

An important clue can be found in the experimental data that monomers of KaiC are

exchanged between KaiC hexamers in the solution of Kai proteins showing the oscillation (21, 24, 26). Ito et al. examined the effects of this monomer shuffling by mixing the oscillatory samples with different phases and found that the synchronization of the oscillation of different samples is mediated by the monomer shuffling during the early dephosphorylation phase (24). We, therefore, may be able to assume that KaiC hexamers can communicate with each other and synchronize their phosphorylation level through the monomer shuffling. In a previous paper, we have conducted a model simulation with a reaction scheme including the monomer shuffling in addition to the allosteric transition of the KaiC hexamer. The result showed that these assumptions are sufficient to sustain the oscillation and to reproduce the experimental data (21) on protein-protein interactions and monomer shuffling semi-quantitatively.

In this paper, robustness of oscillation generated by this mechanism is tested and is compared with experiments. We examine the robustness of oscillation by changing concentrations of Kai proteins and show that our proposed mechanism explains the experimental data on how the oscillation persists in the lower concentrations of Kai proteins. The results also predict the robust oscillation in the higher concentrations of Kai proteins, which should highlight the difference of the present scheme from that based on the other scenario. We also simulate the robustness of the oscillation against the change in the reaction volume down to the size of a sub-cellular domain. Robustness in the small system should shed light on the mechanism of *in vivo* circadian oscillation.

In the following section, we first describe the oscillation observed under the two assumptions of the allosteric transition and the monomer shuffling by using a simplified reaction scheme to illustrate the essential features of thus generated oscillation. Then, to compare the results with experiments quantitatively, the full model with augmented reactions is introduced. With this model, the robustness of the oscillation against the change in the concentration or the reaction volume is discussed. Our assumption of synchronization through the monomer shuffling is compared with other assumptions (26, 27, 32). The last section is devoted to summary and discussion.

TWO BASIC ASSUMPTIONS: A MINIMAL MODEL

As discussed in Introduction, two main assumptions in our model are the allosteric transition of KaiC hexamers and the shuffling of KaiC monomers. In order to illustrate the implication of these assumptions, we first discuss a simplified reaction scheme as shown in Figure 2.

We assume that each KaiC hexamer exhibits the allosteric transition between the relaxed (R) and tense (T) states. Noting the fact that the monomer shuffling is more

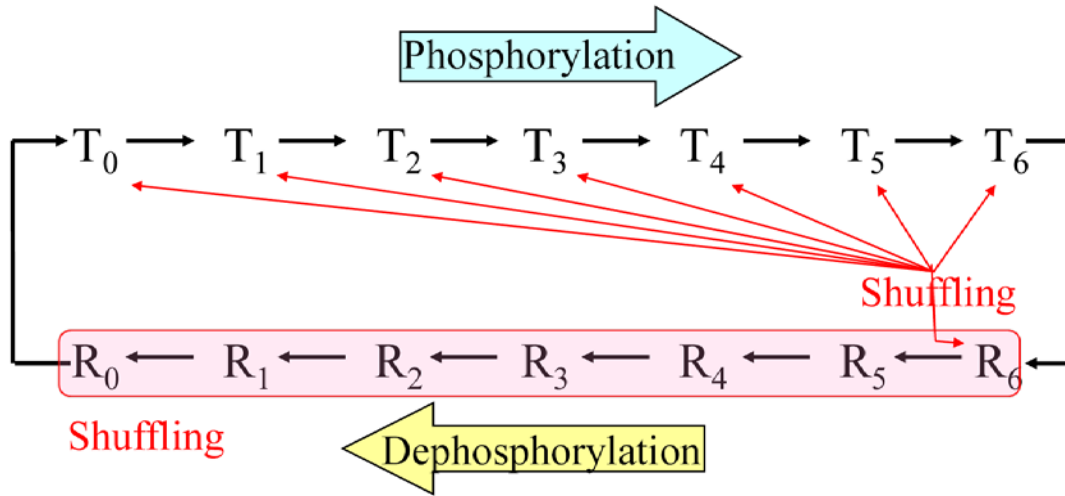


Figure 2

The minimal model assuming both the allosteric transition and the monomer shuffling. Phosphorylation/dephosphorylation and allosteric transitions are indicated by black arrows. The monomer shuffling is allowed between T and R_6 (red arrows) and between two Rs (pink area).

frequent in the dephosphorylation phase than in the phosphorylation phase (21, 24), we may regard that the destabilized KaiC hexamers in the dephosphorylation phase are in the R state, whereas the KaiC hexamers in the phosphorylation phase are in the T state. Each KaiC monomer has two sites to be phosphorylated, Thr432 and Ser431 (5, 6, 23, 25). It was observed that the phosphorylation and dephosphorylation of Thr432 precedes the phosphorylation and dephosphorylation of Ser431 in the oscillation cycle, respectively (23, 25). Though such ordered reactions might play a significant role in generating the rhythm, we here focus, for simplicity, only on Ser431 whose phosphorylation state determines the affinity of KaiC to KaiB (23). Then, the state of each KaiC hexamer is labeled as R_i or T_i , where $i = 0-6$ is the number of monomers with phosphorylated Ser431 in the KaiC hexamer.

KaiA binds to KaiC in the phosphorylation phase, which we identify with the T state. The bound KaiA catalyzes phosphorylation of KaiC (19, 21) as $T_i \rightarrow T_{i+1}$. KaiB, on the other hand, binds to KaiC in the dephosphorylation phase, which we identify with the R state, and the bound KaiB inhibits KaiA from catalyzing the phosphorylation of KaiC (4, 21, 23). When KaiB inhibits KaiA from catalyzing the phosphorylation, i decreases due to the autophosphatase activity of the KaiC hexamer (4, 19, 21) as $R_i \rightarrow R_{i-1}$. In the present simplified version, the reactions involving KaiA or KaiB are not explicitly taken into

account but are effectively represented by the reactions $T_i \rightarrow T_{i+1}$ and $R_i \rightarrow R_{i-1}$. Since rates of phosphorylation and dephosphorylation are similar to each other (21), we here use the same rate constant for both $T_i \rightarrow T_{i+1}$ and $R_i \rightarrow R_{i-1}$. If the rate of transition from T_i to R_i is higher for larger i and the rate of the transition from R_i to T_i is higher for smaller i , the main population would go through the possible states in a circular manner. In the present simplified version, we regard only $T_6 \rightarrow R_6$ and $R_0 \rightarrow T_0$ as the effective routes of transition, which is the simplest realization of the circular reactions.

Since the monomer shuffling becomes more frequent in the dephosphorylation phase (21, 24), we assume the shuffling reactions of $R_i + R_j \rightarrow R_k + R_l$ with $i + j = k + l$, but the less frequent shuffling of $T_i + T_j \rightarrow T_k + T_l$ is not considered here. The monomer shuffling is most frequent at the beginning of the dephosphorylation phase corresponding to the states with large i (24), suggesting that R_i with large i exchanges monomers also with T_j s. In the present simplified model, only the shuffling reactions between R_6 and T_j are considered. It would be reasonable to assume that KaiC hexamers just after the shuffling tend to be destabilized. In the present model, we simply express this tendency by assuming that KaiC hexamers after the shuffling are in the R states. We thus consider the reactions of $R_6 + T_j \rightarrow R_k + R_l$ with $6 + j = k + l$. It should be noted that such shuffling reactions between R_6 and T_j have an autocatalytic character since the population of KaiC in the R states increases with the rate which depends nonlinearly on the concentration of KaiC in the R_6 states.

By denoting the concentration of T_i and R_i as $[T_i]$ and $[R_i]$, respectively, reactions in the model can be represented as follows;

$$\begin{aligned}
\frac{d[T_0]}{dt} &= k_2[R_0] - k_1[T_0] - k_s[T_0][R_6], \\
\frac{d[T_i]}{dt} &= k_1([T_{i-1}] - [T_i]) - k_s[T_i][R_6], \quad \text{for } i = 1-5, \\
\frac{d[T_6]}{dt} &= k_1[R_5] - k_3[T_6] - k_s[T_6][R_6], \\
\frac{d[R_6]}{dt} &= k_3[T_6] - k_1[R_6] - k_s \sum_{j=0}^6 [T_j][R_6] - k_s \sum_{j=0}^5 [R_j][R_6] - 2k_s[R_6]^2 + k_s W_6(\{[R_j]\}, \{[T_j]\}), \\
\frac{d[R_i]}{dt} &= k_1([R_{i+1}] - [R_i]) - k_s \sum_{j=0(j \neq i)}^6 [R_j][R_i] - 2k_s[R_i]^2 + k_s W_i(\{[R_j]\}, \{[T_j]\}), \\
& \hspace{25em} \text{for } i = 1-5, \\
\frac{d[R_0]}{dt} &= k_1[R_1] - k_2[R_0] - k_s \sum_{j=1}^6 [R_j][R_0] - 2k_s[R_0]^2 + k_s W_0(\{[R_j]\}, \{[T_j]\}), \quad (1)
\end{aligned}$$

where $k_s W_i(\{[R_j]\}, \{[T_j]\})$ represents the rate with which R_i is yielded through shuffling reactions. The explicit forms of the bilinear functions, $W_i(\{[R_j]\}, \{[T_j]\})$ with $i = 0-6$, are given in Appendix. The model consists of 14 variables of $\{[R_i]\}$ and $\{[T_i]\}$ and four rate constants, k_1, k_2, k_3 , and k_s , where k_1 is the rate constant of $T_i \rightarrow T_{i+1}$ and $R_i \rightarrow R_{i-1}$, k_2 is the rate constant of $R_0 \rightarrow T_0$, k_3 is the rate constant of $T_6 \rightarrow R_6$, and k_s is the rate constant of shuffling reactions. When we scale the unit of time by $1/k_1$ in Eq.1, we can see that the solution of Eq.1 is determined by three independent parameters, $k_2/k_1, k_3/k_1$, and k_s/k_1 .

It should be noted here that the following two conditions are met in the reaction mixture *in vitro*; The monomer shuffling takes place in a relatively short time scale (21), so that the total rate of shuffling, $\sum_i k_s [R_6] [T_i]$, are higher than the rate of the allosteric transition, $k_3 [T_6]$. On the other hand, as the phosphorylation phase is maintained for a certain duration (23), the rate of the allosteric transition are lower than the rate of phosphorylation. We thus have

$$\begin{aligned} \sum_i k_s [R_6] [T_i] &> k_3 [T_6], \\ k_1 [T_i] &> k_3 [T_6]. \end{aligned} \quad (2)$$

Since the stable oscillation was experimentally observed in a solution containing KaiC monomers of $3.5\mu\text{M}$ (20, 21, 23), the total concentration of KaiC hexamer is fixed to a constant value of $C_0 = \sum_i ([T_i] + [R_i]) = 3.5\mu\text{M} / 6 = 0.58\mu\text{M}$. Considering $[T_i] \approx [T_6]$ and $C_0 > [R_6]$, Eq.2 should lead to the approximate relations,

$$k_s C_0 > k_3, \quad k_1 > k_3. \quad (3)$$

In Figure 3, the simulated temporal change of the phosphorylation level,

$$p(t) = \sum_{i=0}^6 i X_i / \left(6 \sum_{i=0}^6 X_i \right), \quad (4)$$

obtained by numerically integrating Eq.1, is plotted as a function of time, where $X_i =$

$[T_i]+[R_i]$. We should note that even if the individual KaiC hexamers can oscillate their phosphorylation levels, $p(t)$ does not oscillate when the synchronization is not realized among many KaiC hexamers. With the parameters satisfying Eq.3, $p(t)$ in Figure 3 oscillates in a coherent rhythmic manner to show that the simplified scheme as shown in Figure 2 can indeed bring about the synchronization. This synchronization is explained by a series of events occurring in each cycle of the simulated trajectory: First, KaiC accumulates at the T_6 state due to the slow transition from T to R. Then, R_6 begins to increase by the slow transition of $T_6 \rightarrow R_6$ and when the population of R_6 accumulates to some extent, R_i starts to increase rapidly through the autocatalytic reactions of $R_6 + T_j \rightarrow R_k + R_l$. In this way, accumulation of T_6 and its collective transition to R_i s are the mechanism to synchronize the phosphorylation level of many KaiC hexamers.

To elucidate the importance of the above scenario for the oscillation, the results obtained with the parameters that do not satisfy Eq.3 are also shown in Figure 3. For example, if the shuffling is prohibited with $k_s = 0$, then the mechanism of synchronization does not work and the population of KaiC reaches the stationary distribution which is peaked at around T_6 . $p(t)$ is kept high due to the accumulation of KaiC hexamers in the T_6 state. When k_3 is large, on the other hand, the rapid transition from T to R leads to the accumulation of KaiC hexamers in the R states, resulting in a damped oscillation of $p(t)$ which approaches a low constant value. When both conditions of $k_s = 0$ and the large k_3 are imposed, $p(t)$ reaches an intermediate value.

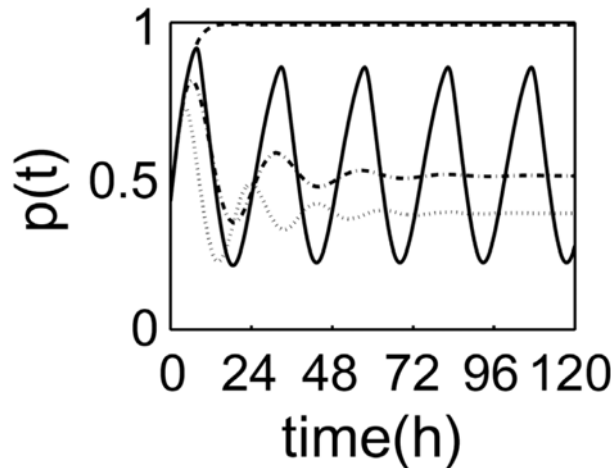


Figure 3

The temporal change of the phosphorylation level $p(t)$ obtained with the minimal model. The solid line is $p(t)$ calculated with the parameterization, $k_2/k_1 = 1$, $k_3/k_1 = 0.001$, and $k_s C_0/k_1 = 10$. $p(t)$ is also simulated by changing one or two of the parameters: the monomer shuffling is prohibited with $k_s = 0$ (dashed line), the allosteric transition from T state to R state is accelerated by increasing k_3 to $k_3/k_1 = 1$ (dotted line), both k_s and k_3 are changed to $k_s = 0$ and $k_3/k_1 = 1$ (dashed-dotted line). Here, k_1 is set to be $1.7 \times 10^{-4} \text{sec}^{-1}$ to fit a period of the real line to the observed value of 22 hours.

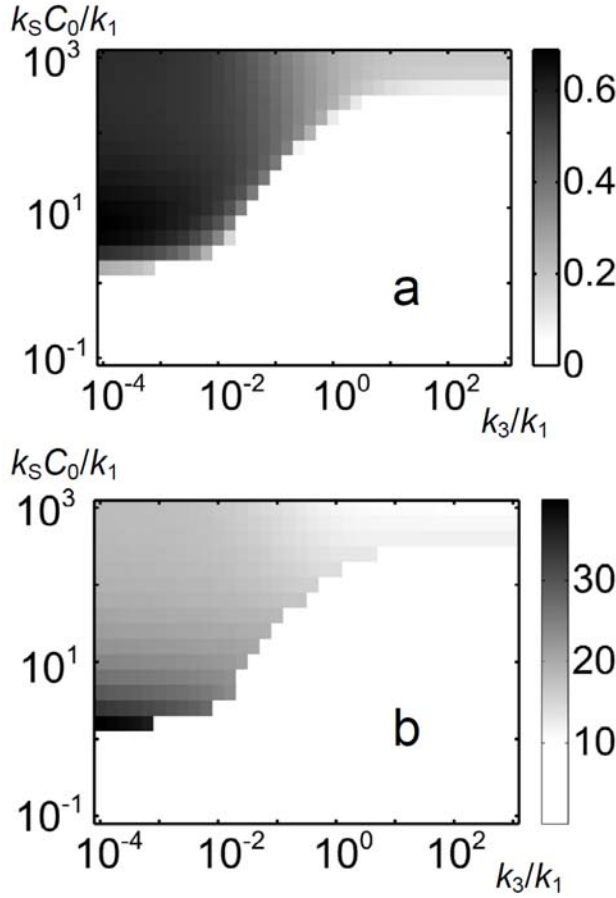


Figure 4

Parameter dependence of solutions of the minimal model. The amplitude (a) and the period length (b) of the oscillation in $p(t)$ are shown on the plane of k_3/k_1 and $k_S C_0/k_1$, where the amplitude is defined as the difference between the maximum and the minimum of oscillating $p(t)$ and the period is shown in unit of hour with $k_1 = 1.7 \times 10^{-4} \text{sec}^{-1}$.

In Figure 4, the amplitude and period of simulated oscillations are shown on the plane of k_3/k_1 , and $k_S C_0/k_1$. The stable oscillation is found in the parameter region satisfying $k_S C_0 > k_1$ and $k_S C_0 \gg k_3$, which is consistent with the condition of Eq.3. Although the rapid oscillation is also possible in the region of $k_1 < k_3$, the amplitude is small compared to the stochastic noise in the more realistic situation which we will discuss later with the full model. Thus, $k_1 > k_3$ is the region where the stability of oscillation is assured. Qualitative features of Figure 4 are not altered by changing k_2/k_1 (data not shown). These results imply that Eq.3 is a necessary condition for the stable oscillation and this should be tested by measuring the rate constants k_S and k_3 of KaiC mutants which have lost the rhythmicity and comparing them with those of the wildtype KaiC.

In this section, the mechanism of synchronization of many KaiC hexamers was proposed and illustrated with a minimal model: KaiC hexamers are synchronized by the autocatalytic reactions working through the combined effects of the slow allosteric transition from T to R and the rapid monomer shuffling between T and R. We have also tested the case in which only the shuffling reactions of $R_i + R_j \rightarrow R_k + R_l$ are allowed but the reactions of $R_6 + T_j \rightarrow R_k + R_l$ are prohibited. $p(t)$ does not oscillate in this case (data

not shown) as expected from the lack of the autocatalytic mechanism. It has been discussed in Ref.26 that the oscillation can be stabilized when the shuffling reactions of $R_i + R_j \rightarrow R_k + R_l$ and $T_i + T_j \rightarrow T_k + T_l$ are allowed but the shuffling reactions between R_i and T_j are prohibited, but with such a constraint on shuffling reactions, we did not find a stable oscillation within our model.

ROBUSTNESS OF OSCILLATION EXAMINED WITH THE FULL MODEL

To quantitatively assess the robustness of oscillation against the changes in concentration of Kai proteins, the reaction schemes of binding and unbinding among Kai proteins should be explicitly defined. In this section we introduce the full model which incorporates these aspects. In our previous paper (28), we have assumed the Michaelis-Menten kinetics for the binding of KaiA or KaiB to KaiC. With the Michaelis-Menten kinetics, however, the rate of binding is insensitive to changes in concentration of KaiA or KaiB, and such modeling of the predefined insensitivity is not suitable for examining the robustness of oscillation. In the present paper, we do not assume the Michaelis-Menten kinetics but describe the binding of KaiA or KaiB to KaiC as stepwise reactions. With this revision, the robustness of oscillation against changes in concentrations of Kai proteins is examined and its prediction is compared with that based on the other model. We also examine the robustness of oscillation in small systems to compare the simulated results with *in vivo* cyanobacterial oscillation.

Full model. KaiA exists as a dimer in solution (11, 14,-16,21), which is denoted here by A_2 . We assume that a KaiA dimer binds to a KaiC hexamer (16, 21) and a KaiB tetramer, which is denoted by B_4 , binds to a KaiC hexamer (17,18). We assume that the binding reactions start with the formation of the encounter complexes, $T_i \tilde{A}_2$, $R_i \tilde{A}_2$, $T_i \tilde{B}_4$, or $R_i \tilde{B}_4$, and then proceed to form the fully bound complexes $T_i A_2$, $R_i A_2$, $T_i B_4$, or $R_i B_4$. KaiA catalyzes the phosphorylation of KaiC (19, 21), and hence the reactions $T_i A_2 \rightarrow T_{i+1} A_2$ and $R_i A_2 \rightarrow R_{i+1} A_2$ are expected. We also consider the ternary complexes, $T_i A_2 \tilde{B}_4$, $R_i A_2 \tilde{B}_4$, $T_i A_2 B_4$ and $R_i A_2 B_4$. The other difference from the model used in the previous paper (28) is on the activity of KaiB: In our previous model, KaiB was assumed to work as a phosphatase with the higher dephosphorylation rate of $R_i B_4 \rightarrow R_{i-1} B_4$ than that in the autophosphatase reaction of $R_i \rightarrow R_{i-1}$. In the present version, we assume that KaiB does not have a strong phosphatase activity but

competitively binds to R_i to decrease the concentration of R_iA_2 , which prevents the kinase reaction of $R_iA_2 \rightarrow R_{i+1}A_2$ as was suggested by experiments (4). See *Appendix* for more detailed description of the model used in this paper.

In the full model, dynamical variables are the concentrations of 86 chemical species and 358 chemical reactions among them are taken into account. In order to simplify the model, we assume that each group of similar chemical reactions have the same rate constant, so that the model has 39 rate constants as summarized in *Supporting Table*. These 39 parameters were chosen to satisfy Eq.2 and Eq.3 to maintain the oscillation and were manually calibrated to reproduce the experimental data for kinetics of reactions among Kai proteins *in vitro* (21): The oscillatory period and phase of amount of various complexes of Kai proteins (Figure 2 of Ref.21), the interaction kinetics of KaiA-KaiC and KaiB-KaiC associations (Figure 4 of Ref.21), and the kinetics of shuffling reactions in different conditions (Figure 5 of Ref.21). The ability of the model to semi-quantitatively reproduce these data was discussed in the previous paper (28). In this paper, the main emphasis lies not on the ability of the model to reproduce those data but on the predictions made by thus defined model on the robustness of oscillation. We discuss later in this section that the predicted robustness is intrinsic to the assumptions made in the model and is in sharp contrast to other models based on the different assumptions.

Stochastic simulation. When the system exhibits stochastic fluctuations, the fluctuations might destroy the coherent oscillation even when the solution of deterministic equations of law of mass action is oscillatory. To examine the robustness of oscillation, therefore, the stochastic simulation is more suited than the deterministic simulation. We here use the Gillespie algorithm (33) to simulate the stochastic chemical reactions defined in Eqs.5-15 in *Appendix*. In stochastic simulation, chemical reactions are represented by changes in numbers of constituting molecules. We refer to the system consisting of $N_A^0 = 10000$ KaiA dimers, $N_B^0 = 30000$ KaiB dimers, and $N_C^0 = 10000$ KaiC hexamers with the system volume $V^0 = 28.5 \text{ fl}$ as the standard mixture, since the reaction mixture having the corresponding concentrations of $1.2\mu\text{M}$ KaiA monomers, $3.5\mu\text{M}$ KaiB monomers, and $3.5\mu\text{M}$ KaiC monomers has been often used in *in vitro* experiments (20, 21, 23). As shown later in this paper, the oscillation in the small system of $V^0 = 28.5 \text{ fl}$ is stable

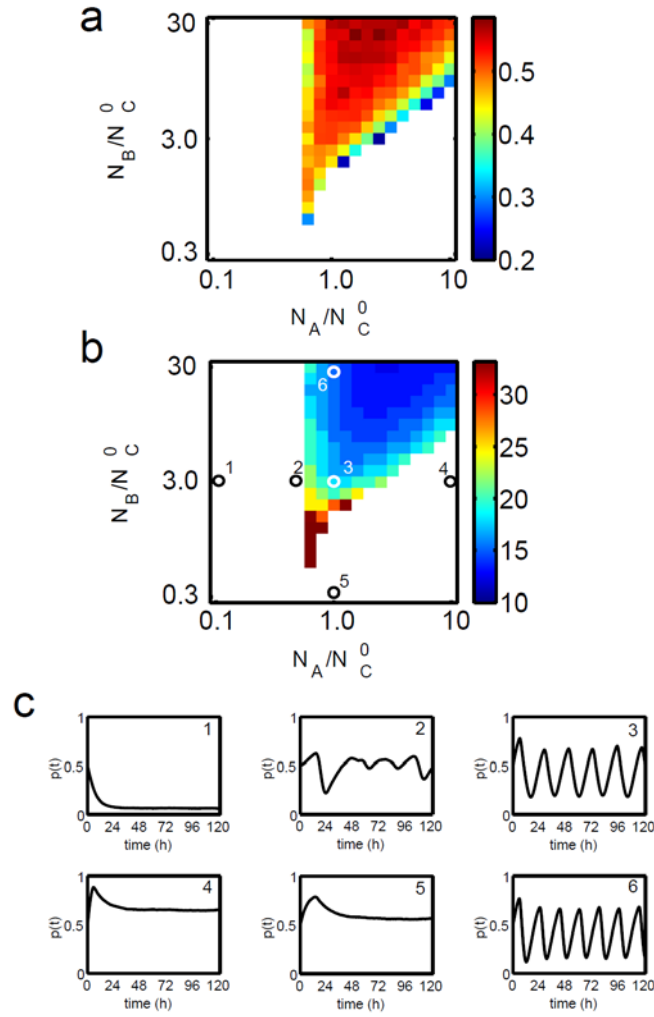


Figure 5

Robustness of the oscillation against changes in concentration of KaiA and KaiB examined with the full model. The amplitude (a) and the period length (b) of the oscillation in $p(t)$ are shown on the plane of N_A/N_C^0 and N_B/N_C^0 , where the amplitude is defined as the difference between the maximum and the minimum of oscillating $p(t)$ and the period is shown in unit of hour. The numbered panel in c shows the trajectory of $p(t)$ calculated with the parameter sets corresponding to the numbered position in b: $N_A = 0.126N_A^0$ and

$$N_B = N_B^0 \quad (1), \quad N_A = 0.5N_A^0 \quad \text{and} \quad N_B = N_B^0 \quad (2), \quad N_A = N_A^0 \quad \text{and} \quad N_B = N_B^0 \quad (3),$$

$$N_A = 7.94N_A^0 \quad \text{and} \quad N_B = N_B^0 \quad (4), \quad N_A = N_A^0 \quad \text{and} \quad N_B = 0.126N_B^0 \quad (5), \quad \text{and} \quad N_A = N_A^0$$

$$\text{and} \quad N_B = 7.94N_B^0 \quad (6).$$

enough to be comparable with the *in vitro* experiments. In the following, we first examine the robustness of oscillation by changing the number of KaiA dimers, N_A , the number of KaiB dimers, N_B , or the number of KaiC hexamers, N_C , by keeping the volume at the standard value of $V = V^0$. We also examine later the robustness of oscillation against change in V by keeping concentrations at the values of the standard mixture as $N_A/V = N_A^0/V^0$, $N_B/V = N_B^0/V^0$, and $N_C/V = N_C^0/V^0$. The total concentration of KaiC hexamer in the phosphorylation level i is calculated as $X_i = [T_i] + [T_i\tilde{A}_2] + [T_iA_2] + [T_i\tilde{B}_4] + [T_iB_4] + [T_iA_2\tilde{B}_4] + [T_iA_2B_4] + [R_i] + [R_i\tilde{A}_2] + [R_iA_2] + [R_i\tilde{B}_4] + [R_iB_4] + [R_iA_2\tilde{B}_4] + [R_iA_2B_4]$ and the phosphorylation level, $p(t)$, is calculated by Eq.4 using thus defined X_i .

Robustness of oscillation against changes in concentration of Kai proteins. In the simulation of the standard mixture with $N_A = N_A^0$, $N_B = N_B^0$ and $N_C = N_C^0$, $p(t)$ shows a regular coherent oscillation as shown in Fig.5c. To examine the robustness of this oscillation against the changes in N_A and N_B with fixed KaiC concentration of $N_C = N_C^0$ and fixed volume of $V = V^0$, the simulated amplitude and period of oscillation are shown on the plane of N_A/N_C^0 and N_B/N_C^0 in Figures 5a and 5b. On this plane, there is a distinct region in which the stable coherent oscillation is realized. In the outside of this region, the oscillation dies out in a manner specific for each set of concentrations as shown in Figure 5c. When N_A/N_C^0 is small, for example, $p(t)$ reaches a low stationary value due to the insufficient concentration of KaiA for phosphorylating KaiC in the T state. The boundary between the oscillatory region and the region of damped $p(t)$ is at around $N_A/N_C^0 \approx 0.5-0.6$, which is consistent with the experimental observation (21). In the region just outside of this boundary, $p(t)$ exhibits chaotic behavior. When N_A/N_C^0 is large, on the other hand, the model predicts that $p(t)$ approaches a

high stationary value. This is because KaiA exceeds the amount to be inhibited by KaiB, which leads to the sustained highly phosphorylated state of KaiC in the R state. $p(t)$ also reaches a large stationary value when N_B is too small to inhibit the effect of KaiA on KaiC in the R state. When concentration of KaiA is fixed to be $N_A = N_A^0$, the boundary between the oscillatory region and the stationary region is at around $N_B/N_C^0 \approx 1.9$, which is consistent with the experimental observation (21). In contrast, the model predicts that the oscillation is kept stable for large N_B unless the reactions neglected in the model, which would become significant when the concentration of KaiB is very large, could intervene the oscillation. This insensitivity to the increase in the KaiB concentration implies that the stronger inhibition of KaiA activity in the R state due to the larger amount of KaiB does not prevent the system from generating the coherent oscillation.

Thus, we showed that the oscillation is robust over the wide ranges of concentrations: When concentrations of KaiB and KaiC are fixed to be $N_B = N_B^0$ and $N_C = N_C^0$, the oscillation is stable for $0.6 < N_A/N_C < 3.0$, and when concentrations of KaiA and KaiC are fixed to be $N_A = N_A^0$ and $N_C = N_C^0$, the oscillation is stable for $1.9 < N_B/N_C$. The model also predicts that the oscillation is robust when N_A and N_B are increased simultaneously. In this case, the effects of the increase of N_A on KaiC in the R state are compensated by the increase of N_B , so that the rate of dephosphorylation of KaiC in the R state is not diminished by the large amount of KaiA.

Robustness was also examined when N_A , N_B , and N_C are scaled uniformly as $N_A = \alpha N_A^0$, $N_B = \alpha N_B^0$, and $N_C = \alpha N_C^0$. Simulated trajectories of $p(t)$ are shown in Figure 6. Oscillation is stable for large α , which is consistent with the observed results (21). When α is small, on the other hand, the rates of phosphorylation and dephosphorylation become low and Eq.1b is not satisfied, with which the stable phosphorylation phase or dephosphorylation phase can not be maintained. The disappearance of the oscillation in the small- α condition is consistent with the

experimental data (21).

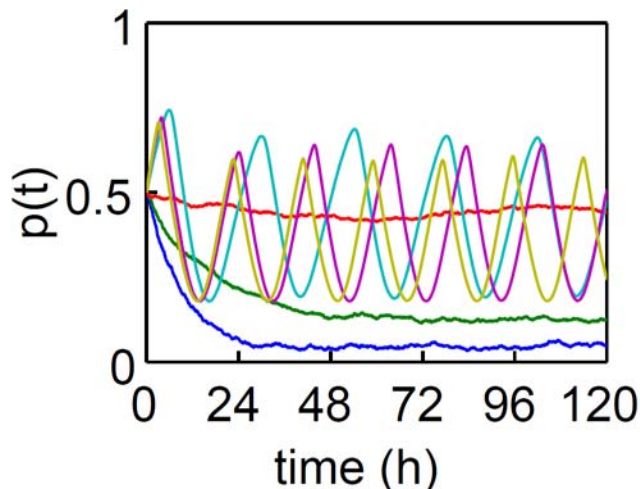


Figure 6

Concentration dependent changes of $p(t)$ calculated with the full model. $p(t)$ for the standard mixture with $\alpha=1$ (light blue), and $p(t)$ for $\alpha=5.0$ (yellow), $\alpha=2.5$ (purple), $\alpha=0.1$ (red), $\alpha=0.05$ (green), and $\alpha=0.025$ (blue).

Comparison with the other scenario. Robustness of the oscillation demonstrated above gives a useful clue to distinguish the different explanations on the mechanism to generate the rhythm. A simple assumption other than the present assumption of monomer shuffling was put forward by van Zon *et al.* (27) and Takigawa-Imamura and Mochizuki (32). In their assumption, KaiA unbinds more slowly from the less phosphorylated KaiC or KaiA binds more rapidly to the less phosphorylated KaiC, which leads to the differential affinity of KaiA to KaiC. When the KaiA concentration is low, this assumption brings about the shortage of KaiA that can bind to the highly phosphorylated KaiC, which leads to the rapid phosphorylation of the less phosphorylated KaiC. The population of the highly phosphorylated KaiC then accumulates to lead to the synchronization.

We should note that this mechanism of synchronization works only when the amount of free unbound KaiA is small enough to bring about the shortage of KaiA that can bind to the highly phosphorylated KaiC. Indeed, the synchronization is realized in our model by tuning parameters to allow the differential affinity and by prohibiting the monomer shuffling, but the stable oscillation is realized only when N_A is as small as $0.1 N_A^0$. van Zon *et al.* (27) have introduced the complex $R_i A_4 B_4$ in their model ($A_2 B_2 \bar{C}_i$ in the

notation of Ref.27), which should absorb the extra free KaiA without much affecting the kinase/phosphatase kinetics to allow the oscillation under the condition of $N_A \approx N_A^0$. Consistent explanation based on the assumption of differential affinity, therefore, requires existence of the effective absorber of KaiA such as the $R_iA_4B_4$ complex. However, since the extra amount of free KaiA inhibits the synchronization, the oscillation based on differential affinity is fragile when the concentration of KaiA is increased. In Figure 6 of Ref.27, the predicted range of the stable oscillation is $0.4 < N_A/N_C < 1.2$, which is apparently different from the wider range of oscillation $0.6 < N_A/N_C < 3.0$ predicted by the present model. A clearer difference is found when both concentration of KaiA and concentration of KaiB are increased at the same time: In Figure 6 of Ref.27, the predicted range of the stable oscillation does not much depend on the concentration of KaiB and stays as $0.4 < N_A/N_C < 1.2$, which is in sharp contrast to the broadened range of oscillation $0.6 < N_A/N_C < 7.9$ with the increased KaiB concentration of $N_B \approx 2N_B^0$ in the present model.

Robustness of oscillation against change in the system volume. Since the cell-cell communication is negligible among cultivated cyanobacterial cells, the observed oscillation of the cyanobacterial clock is the feature of individual cell, which is generated by the intracellular biochemical network (34). Although the circadian rhythm can be reconstituted *in vitro*, the system volume is quite different between *in vitro* and *in vivo* experiments. In the presence of the *in vitro* reconstituted oscillation, one may expect that the same mechanism as in the *in vitro* system works to stabilize the cyanobacterial circadian rhythms *in vivo*. As the system volume becomes smaller down to the cell size, however, the smallness of numbers of molecules in the system should bring about stochastic fluctuations in chemical reactions, which may randomly perturb dynamics to make the oscillation irregular. This raises an important question on whether the reconstituted *in vitro* oscillation can be persistent when the system volume is decreased down to the cellular or sub-cellular size.

We test the persistency of the oscillation by changing the system volume as βV^0 and the number of Kai proteins $N_A = \beta N_A^0$, $N_B = \beta N_B^0$, and $N_C = \beta N_C^0$ with $\beta < 1$,

while keeping the concentrations constant. Persistency of the oscillation in small systems is assessed by measuring the correlation number of cycle, $n_{1/2}$, in the simulated trajectories as follows. Starting from the same initial condition, the time evolution of $p(t)$ in $N = 50$ systems are simulated by N trajectories obtained with different random number seeds. In the i th trajectory of simulation, $p(t)$ shows the n th peak at time $t = t_i(n)$. Since a first few simulated cycles are transient cycles leaving the features of the initial condition, the data of the first two cycles are not used in taking average, so that the time duration for n cycles is defined by $T_i(n) = t_i(n+2) - t_i(2)$. For N trajectories, we

calculate the average time duration for n cycles $T(n) = (1/N) \sum_{i=1}^N T_i(n)$ and its variance

over different trajectories $\sigma(n)^2 = (1/N) \sum_{i=1}^N (T_i(n) - T(n))^2$. When the oscillation is

stable, the averaged period length, $L = T(n)/n$, is almost independent of n . In Figure 7, the normalized variance, $\sigma(n)^2 / L^2$ is plotted as a function of n , showing that $\sigma(n)^2$ increases approximately linearly as n increases. The linear dependence of $\sigma(n)^2$ on n indicates that the oscillatory phase shifts stochastically as a random walk in each trajectory. The slope of $\sigma(n)^2 / L^2$ is steeper as β is smaller, showing that the fluctuation in the oscillatory phase is increased as the system volume is decreased.

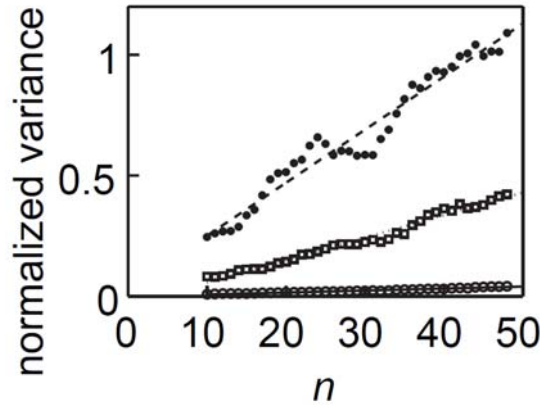


Figure 7

The normalized variance of trajectory-to-trajectory fluctuation of the time length of n cycles, $\sigma(n)^2 / L^2$, calculated with the full model is plotted as a function of n .

$\beta = N_A / N_A^0 = N_B / N_B^0 = N_C / N_C^0 = V / V^0 = 0.398$ (open circles), 0.04 (open squares), and

0.0125 (filled circles) with $N_A^0 = 10000$, $N_B^0 = 30000$, $N_C^0 = 10000$, and $V^0 = 28.5fl$. The

dashed line is a guide for eyes.

As a measure of the timescale for the loss of correlation among different trajectories, we define the correlation number of cycle $n_{1/2}$ by $\sigma(n = n_{1/2})^2 / L^2 = (0.5)^2$. In other words, as $n_{1/2}$ days have passed, the trajectory-to-trajectory fluctuation has accumulated to be a half day. In Figure 8, $n_{1/2}$ is plotted as a function of β . The oscillation is remarkably persistent as $n_{1/2} > 100$ cycles for $\beta > 0.1$. This indicates that the *in vitro* oscillation is quite robust down to the cell size $V = \beta V^0 \approx 1\sim 2$ fl. Though N_C is as large as $N_C \approx 1000\sim 2000$ (6000~12000 monomers of KaiC) in a cyanobacterial cell (4), N_A was reported to be as small as $N_A \approx 120\sim 250$ (240~500 monomers of KaiA) in a cell (4). With this small N_A , the reactions have to be confined in a small subcellular region to keep the same concentration as in the standard mixture with $\beta = N_A / N_A^0 = V / V^0 \approx 0.012\sim 0.025$. For such a small system, $n_{1/2}$ is approximately 10 cycles. In experiment, the correlation time during which the cyanobacterial oscillation is persistent is 166 ± 100 days (35). If the whole bacterial cell volume is used to generate the

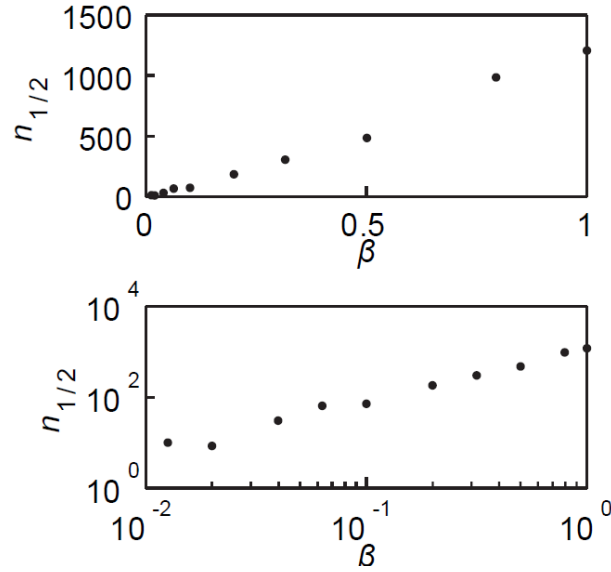


Figure 8

The correlation number of cycles, $n_{1/2}$, calculated with the full model is plotted as a function of $\beta = N_A / N_A^0 = N_B / N_B^0 = N_C / N_C^0 = V / V^0$ with $N_A^0 = 10000$, $N_B^0 = 30000$, $N_C^0 = 10000$, and $V^0 = 28.5$ fl. The upper figure is plotted in the linear scale and the lower figure is in the log-log scale.

oscillation with $N_C \approx 1000\sim 2000$, $n_{1/2}$ in simulation is comparable with the correlation time observed *in vivo*, and hence the mechanism of the *in vitro* oscillation can sustain the observed single-cell oscillation. If only the subcellular domain is responsible for the oscillation with $N_A \approx N_C \approx 120\sim 250$ as was suggested in Ref.4, then the persistency of the *in vitro* oscillation is not enough to explain the observed correlation time and the transcriptional-translational feedback mechanism may be needed to complement the persistency. Further theoretical and experimental characterization should help to clarify the relative importance of the robustness provided by three proteins within the observed robustness *in vivo*.

SUMMARY AND DISCUSSION

In this paper, we examined the robustness of oscillation generated by the combined effects of the allosteric transition and the monomer shuffling. When the concentration of Kai proteins is decreased, the oscillation generated by this mechanism dies out as was observed in experiments. The model predicted that the oscillation is robust over the wide range of N_A/N_C , which should highlight the difference of the proposed mechanism from the mechanism based on the differential affinity. The model also predicted that the oscillation is robust when the system volume is decreased to the cellular size, but when the volume is decreased down to the subcellular size, the other mechanism should be required to explain the observed persistency of the *in vivo* oscillation.

The mechanism presented here may be further extended to conform to the observation that KaiC has two sites, Thr432 and Ser431, to be phosphorylated. When we write the phosphorylated Thr432 and Ser 431 as pT and pS, and nonphosphorylated Thr432 and Ser 431 as T and S, respectively, recent experiments revealed that KaiC undergoes a definite sequence of states as $T/S \rightarrow pT/S \rightarrow pT/pS \rightarrow T/pS \rightarrow T/S$ in every cycle of oscillation (23, 25).

Rust *et al.* proposed the scenario (25) that KaiC hexamers can be synchronized without relying on the monomer shuffling mechanism by using the sequential process of phosphorylation/dephosphorylation of T and S. Their proposed mechanism is based on the following assumptions (1) The autophosphatase reaction of $pT/pS \rightarrow T/pS$ is slow and KaiC is accumulated at the pT/pS state because KaiA catalyses the reverse reaction of $pT/pS \leftarrow T/pS$. (2) KaiB does not bind to pT/pS but binds to T/pS. (3) The KaiB-KaiC complex formed in the T/pS state inhibits the activity of KaiA through the formation of KaiABC complex. With these assumptions, KaiC hexamers accumulated in the pT/pS state are collectively transformed to the T/pS state due to the autocatalytic inhibition of

the $pT/pS \leftarrow T/pS$ reaction through binding of KaiB to KaiC in the T/pS state, and hence the oscillatory phase of KaiC is synchronized. These assumptions, however, seem to be in contradiction to the experimental observation (23) suggesting that (1') The autophosphatase reaction of $pT/pS \rightarrow T/pS$ is fast and the rate is not affected by the presence or absence of KaiA or KaiB. (2') KaiB binds both to pT/pS and T/pS with the similar binding affinity. (3') KaiB inhibits the reverse reaction of $T/pS \leftarrow T/S$ but does not inhibit other reactions significantly. Therefore, at the present stage, we have no consistent model to explain all the reported experimental data and it is especially important to examine whether the mechanism of monomer shuffling proposed in this paper is consistent with the observed data of sequential phosphorylation/dephosphorylation of two sites.

Another important experimental finding is the recent measurement of the ATP hydrolysis reactions catalyzed by KaiC (22). By comparing KaiC mutants, the strong correlation was found between the rate of ATP hydrolysis and the frequency (the inverse of the period length) of the oscillation of the phosphorylation level of KaiC. It is also notable that the rate of ATP hydrolysis is temperature compensated (22). These data strongly suggest that the ATP hydrolysis catalyzed by KaiC is the fundamental reaction which determines the time constant of *in vitro* circadian oscillation. Thus, we now have two basic questions on the mechanism of oscillation of the Kai protein system: One is on the mechanism of the temperature compensated ATP hydrolysis reaction, which determines the fundamental time constant of the KaiC oscillation. A thermodynamic description of the ATP hydrolysis and coupled structural changes should help to clarify the molecular interactions which bring about the temperature compensation. The other is on the mechanism of the synchronization of many KaiC molecules. Although we have discussed only the latter in the present paper, these two problems should be interrelated to each other. Synergetic approaches of both theoretical modeling and experiments should be necessary to find a unified view on these two problems.

ACKNOWLEDGEMENT

The authors acknowledge fruitful discussion with Dr. Kondo and his colleagues. The authors also thank Dr. Mihalcescu for discussion on the effects of smallness of the system size. This work was supported by grants from the Ministry of Education, Culture, Sports, Science, and Technology, Japan, and by grants for the 21st century COE program for Frontiers of Computational Science.

APPENDIX

Bilinear functions in the minimal model. In Eq.1, the bilinear functions $W_i(\{[R_j]\}, \{[T_j]\})$, which determine the rate of yielding R_i through shuffling reactions, are defined as

$$\begin{aligned} W_0(\{[R_j]\}, \{[T_j]\}) = & C_{60}([T_0] + [R_0])[R_6] + (C_{60}[R_1] + C_{50}[R_0])[R_5] \\ & + (C_{60}[R_2] + C_{50}[R_1] + C_{40}[R_0])[R_4] + (C_{60}[R_3] + C_{50}[R_2] + C_{40}[R_1] + C_{30}[R_0])[R_3] \\ & + (C_{40}[R_2] + C_{30}[R_1] + C_{20}[R_0])[R_2] + (C_{20}[R_1] + [R_0])[R_1] + 2[R_0]^2, \end{aligned}$$

$$\begin{aligned} W_1(\{[R_j]\}, \{[T_j]\}) = & (C_{50}[T_1] + C_{61}[T_0] + C_{50}[R_1] + C_{61}[R_0])[R_6] \\ & + (C_{50}[R_2] + C_{61}[R_1] + C_{51}[R_0])[R_5] + (C_{50}[R_3] + C_{61}[R_2] + C_{51}[R_1] + C_{41}[R_0])[R_4] \\ & + (C_{61}[R_3] + C_{51}[R_2] + C_{41}[R_1] + C_{31}[R_0])[R_3] + (C_{41}[R_2] + C_{31}[R_1] + 2C_{21}[R_0])[R_2] \\ & + (2C_{21}[R_1] + [R_0])[R_1], \end{aligned}$$

$$\begin{aligned} W_2(\{[R_j]\}, \{[T_j]\}) = & (C_{40}[T_2] + C_{51}[T_1] + C_{62}[T_0] + C_{40}[R_2] + C_{51}[R_1] + C_{62}[R_0])[R_6] \\ & + (C_{40}[R_3] + C_{51}[R_2] + C_{62}[R_1] + C_{52}[R_0])[R_5] \\ & + (C_{40}[R_4] + C_{51}[R_3] + C_{62}[R_2] + C_{52}[R_1] + 2C_{42}[R_0])[R_4] \\ & + (C_{62}[R_3] + C_{52}[R_2] + 2C_{42}[R_1] + C_{31}[R_0])[R_3] + (2C_{42}[R_2] + C_{31}[R_1] + C_{20}[R_0])[R_2] \\ & + C_{20}[R_1]^2, \end{aligned}$$

$$\begin{aligned} W_3(\{[R_j]\}, \{[T_j]\}) = & (C_{30}[T_3] + C_{41}[T_2] + C_{52}[T_1] + 2C_{63}[T_0])[R_6] \\ & + (C_{30}[R_3] + C_{41}[R_2] + C_{52}[R_1] + 2C_{63}[R_0])[R_6] \\ & + (C_{30}[R_4] + C_{41}[R_3] + C_{52}[R_2] + 2C_{63}[R_1] + C_{52}[R_0])[R_5] \\ & + (C_{41}[R_4] + C_{52}[R_3] + 2C_{63}[R_2] + C_{52}[R_1] + C_{41}[R_0])[R_4] \\ & + (2C_{63}[R_3] + C_{52}[R_2] + C_{41}[R_1] + C_{30}[R_0])[R_3] + (C_{41}[R_2] + C_{30}[R_1])[R_2], \end{aligned}$$

$$\begin{aligned} W_4(\{[R_j]\}, \{[T_j]\}) = & (C_{20}[T_4] + C_{31}[T_3] + 2C_{42}[T_2] + C_{52}[T_1] + C_{62}[T_0])[R_6] \\ & + (C_{20}[R_4] + C_{31}[R_3] + 2C_{42}[R_2] + C_{52}[R_1] + C_{62}[R_0])[R_6] \\ & + (C_{20}[R_5] + C_{31}[R_4] + 2C_{42}[R_3] + C_{52}[R_2] + C_{62}[R_1] + C_{51}[R_0])[R_5] \\ & + (2C_{42}[R_4] + C_{52}[R_3] + C_{62}[R_2] + C_{51}[R_1] + C_{40}[R_0])[R_4] \\ & + (C_{62}[R_3] + C_{51}[R_2] + C_{40}[R_1])[R_3] + C_{40}[R_2]^2, \end{aligned}$$

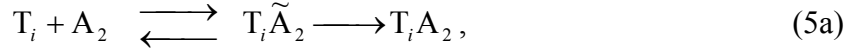
$$\begin{aligned}
W_5(\{[R_j]\}, \{[T_j]\}) &= ([T_5] + 2C_{21}[T_4] + C_{31}[T_3] + C_{41}[T_2] + C_{51}[T_1] + C_{61}[T_0])[R_6] \\
&+ ([R_5] + 2C_{21}[R_4] + C_{31}[R_3] + C_{41}[R_2] + C_{51}[R_1] + C_{61}[R_0])[R_6] \\
&+ (2C_{21}[R_5] + C_{31}[R_4] + C_{41}[R_3] + C_{51}[R_2] + C_{61}[R_1] + C_{50}[R_0])[R_5] \\
&+ (C_{41}[R_4] + C_{51}[R_3] + C_{61}[R_2] + C_{50}[R_1])[R_4] + (C_{61}[R_3] + C_{50}[R_2])[R_3], \\
W_6(\{[R_j]\}, \{[T_j]\}) &= (2[T_6] + [T_5] + C_{20}[T_4] + C_{30}[T_3] + C_{40}[T_2] + C_{50}[T_1] + C_{60}[T_0])[R_6] \\
&+ (2[R_6] + [R_5] + C_{20}[R_4] + C_{30}[R_3] + C_{40}[R_2] + C_{50}[R_1] + C_{60}[R_0])[R_6] \\
&+ (C_{20}[R_5] + C_{30}[R_4] + C_{40}[R_3] + C_{50}[R_2] + C_{60}[R_1])[R_5] \\
&+ (C_{40}[R_4] + C_{50}[R_3] + C_{60}[R_2])[R_4] + C_{60}[R_3]^2,
\end{aligned}$$

where C_{ij} are factors representing the probability to choose j monomers from i monomers;

$$\begin{aligned}
C_{20} &= \frac{{}_2C_0}{{}_2C_0 + {}_2C_1} = \frac{1}{3}, \quad C_{21} = \frac{{}_2C_1}{{}_2C_0 + {}_2C_1} = \frac{2}{3}, \quad C_{30} = \frac{{}_3C_0}{{}_3C_0 + {}_3C_1} = \frac{1}{4}, \quad C_{31} = \frac{{}_3C_1}{{}_3C_0 + {}_3C_1} = \frac{3}{4}, \\
C_{40} &= \frac{{}_4C_0}{{}_4C_0 + {}_4C_1 + {}_4C_2} = \frac{1}{11}, \quad C_{41} = \frac{{}_4C_1}{{}_4C_0 + {}_4C_1 + {}_4C_2} = \frac{4}{11}, \quad C_{42} = \frac{{}_4C_2}{{}_4C_0 + {}_4C_1 + {}_4C_2} = \frac{6}{11}, \\
C_{50} &= \frac{{}_5C_0}{{}_5C_0 + {}_5C_1 + {}_5C_2} = \frac{1}{16}, \quad C_{51} = \frac{{}_5C_1}{{}_5C_0 + {}_5C_1 + {}_5C_2} = \frac{5}{16}, \quad C_{52} = \frac{{}_5C_2}{{}_5C_0 + {}_5C_1 + {}_5C_2} = \frac{10}{16}, \\
C_{60} &= \frac{{}_6C_0}{{}_6C_0 + {}_6C_1 + {}_6C_2 + {}_6C_3} = \frac{1}{42}, \quad C_{61} = \frac{{}_6C_1}{{}_6C_0 + {}_6C_1 + {}_6C_2 + {}_6C_3} = \frac{6}{42}, \\
C_{62} &= \frac{{}_6C_2}{{}_6C_0 + {}_6C_1 + {}_6C_2 + {}_6C_3} = \frac{15}{42}, \quad C_{63} = \frac{{}_6C_3}{{}_6C_0 + {}_6C_1 + {}_6C_2 + {}_6C_3} = \frac{20}{42}.
\end{aligned}$$

Full model with the stepwise binding. We assume that KaiA and KaiC first form an encounter complex of $T_i\tilde{A}_2$ and then proceed to form a fully bound complex of T_iA_2 .

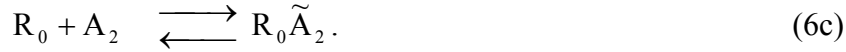
We also assume that the free energy barrier between T_iA_2 and $T_i\tilde{A}_2$ is higher than that between $T_i\tilde{A}_2$ and $T_i + A_2$, so that T_iA_2 can directly dissociate into $T_i + A_2$ without being trapped into $T_i\tilde{A}_2$. We have, therefore,



Similarly, for $i = 1-6$, R_i and KaiA bind in a stepwise way and dissociate in a direct way as



We assume that KaiA does not bind strongly to R_0 , so that we have



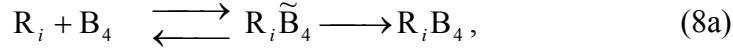
Eq.6c inherits the assumption used in the model of the previous paper (28). Since phosphorylation of R_0 competes with the allosteric transition at R_0 , the reaction scheme had to be calibrated to control the transition rate by excluding $R_0 A_2$ from the model. This calibration was necessary to quantitatively explain the experimental data on the temporal evolution of the shuffling reactions (Figure 8 of Ref.28). We should note that for the simulation of the present paper, the lack of $R_0 A_2$ in the model gives little influence to the quantitative results.

KaiB forms a dimer in solution (11, 21) and KaiC may bind to a tetrameric form of KaiB (17,18). In this model, we assume that dimers and tetramers of KaiB are at equilibrium in solution as

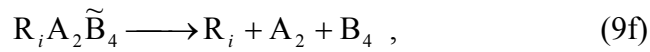
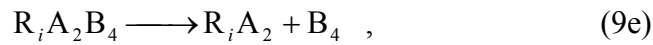
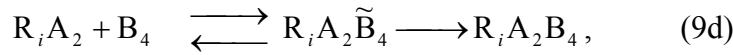
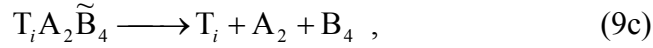
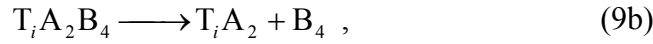
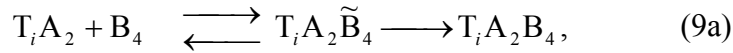


and KaiC binds to the tetrameric form of KaiB. Since the concentration of the KaiB-KaiC

complex was observed to be high in the dephosphorylation phase (21), we assume the stepwise binding process of R_i and KaiB as

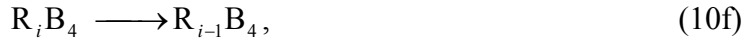
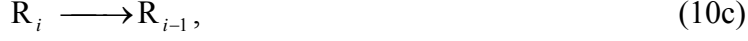


In the reaction mixture containing KaiA, KaiB and KaiC, it was observed that the KaiC-KaiA-KaiB tertiary complex is formed both in the phosphorylation and dephosphorylation phases (21), so that we assume



where Eqs.9c and 9f are based on the assumption that the weak binding of KaiB to the KaiC-KaiA complex does not alter the chemical properties of KaiC-KaiA complex, so that KaiC-KaiA complex dissociates into KaiC and KaiA in the same way as in Eqs.5b and 6b. Due to the autophosphatase activity of KaiC, the phosphorylation level is decreased in the absence of the strongly bound KaiA;





where Eqs.10b and 10d are based on the assumption that the weakly bound KaiA in the encounter complex does not catalyze the phosphorylation and KaiC is dephosphorylated in the same way as in Eqs.10a and 10c. In the previous paper (28), we assumed that KaiC is dephosphorylated with a high rate in the KaiC-KaiB complex, but here we assume that KaiB only hinders the binding of KaiA and the rates of the reactions in Eqs.10e and 10f are assumed to be same as that of Eq.10c. Such a role of KaiB was suggested by experiments (4).

When KaiA binds strongly to KaiC in fully bound complex, KaiA catalyzes phosphorylation of KaiC. We assume that the kinase activity of KaiA is not diminished when KaiB additionally binds to the KaiC-KaiA complex through Eqs.9a and 9d;

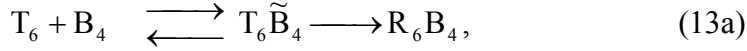


The allosteric transition from R to T is assumed to be induced also from the weakly

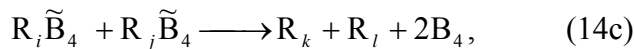
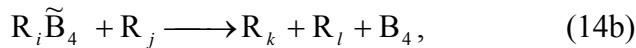
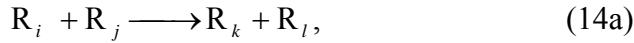
bound encounter complexes as

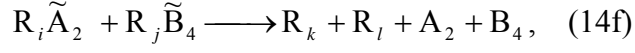
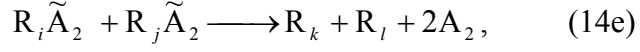
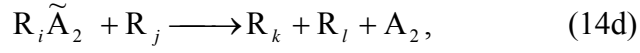


In Eq.12 we assumed that the transition from R_0 to T_0 occurs spontaneously with the slower reverse transition from T_0 to R_0 , but the transition from T_6 to R_6 should not be so fast to maintain the oscillation as explained in the section of *Two Basic Assumptions: A Minimal Model*. We express this slow transition from T_6 to R_6 by imposing the constraint that the transition is triggered by the binding of KaiB to T_6 as

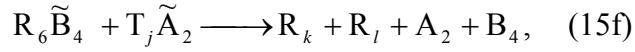
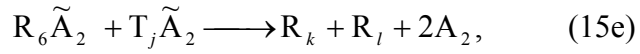
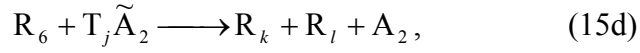
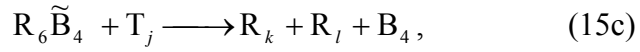
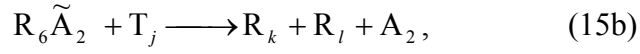
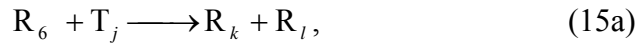


where Eq.13b is based on the assumption that the weakly bound KaiA does not affect reactions much and the reactions concerning the encounter complex with weakly bound KaiA is similar to those in the KaiA-free state as in Eq.13a. The shuffling reactions are assumed to be similar to those in the simplified version of the section of *Two Basic Assumptions: A Minimal Model*;





with $i + j = k + l$, and



with $6 + j = k + l$. Here, Eqs.14b-14f and Eqs.15b-15f are based on the assumption that the weak binding of KaiA or KaiB to KaiC does not affect the shuffling reactions. Eqs.5-15 define the reaction schemes of the full model in the present paper. The parameters used in Eqs.5-15 are summarized in *Supplementary Table*.

REFERENCES

1. Ishiura, M., S. Kutsuna, S. Aoki, H. Iwasaki, C. R. Andersson, A. Tanabe, S. S. Golden, C. H. Johnson, and T. Kondo. 1998. Expression of a gene cluster *kaiABC* as a circadian feedback process in cyanobacteria. *Science*. 281:1519-1523.
2. Iwasaki, H., Y. Taniguchi, M. Ishiura, and T. Kondo. 1999. Physical interactions among circadian clock proteins KaiA, KaiB and KaiC in cyanobacteria. *EMBO J*. 18:1137-1145.
3. Nishiwaki, T., H. Iwasaki, M. Ishiura, and T. Kondo. 2000. Nucleotide binding and autophosphorylation of the clock protein KaiC as a circadian timing process of cyanobacteria, *Proc. Natl. Acad. Sci. USA*. 97:495-499.
4. Kitayama, Y., H. Iwasaki, T. Nishiwaki, and T. Kondo. 2003. KaiB functions as an attenuator of KaiC phosphorylation in the cyanobacterial circadian clock system. *EMBO J*. 22:2127-2134.
5. Nishiwaki, T., Y. Satomi, M. Nakajima, C. Lee, R. Kiyohara, H. Kageyama, Y. Kitayama, M. Temamoto, A. Yamaguchi, A. Hijikata, M. Go, H. Iwasaki, T. Takao, and T. Kondo. 2004. Role of KaiC phosphorylation in the circadian clock system of *Synechococcus elongatus* PCC 7942. *Proc. Natl. Acad. Sci. USA*. 101:13927-13932.
6. Xu, Y., T. Mori, R. Pattanayek, S. Pattanayek, M. Egli, and C. H. Johnson. 2004. Identification of key phosphorylation sites in the circadian clock protein KaiC by crystallographic and mutagenetic analyses. *Proc. Natl. Acad. Sci. USA*. 101:13933-13938.
7. Mori, T., S. V. Saveliev, Y. Xu, W. F. Stafford, M. M. Cox, R. B. Inman, and C. H. Johnson. 2002. Circadian clock protein KaiC forms ATP-dependent hexameric rings and binds DNA. *Proc. Natl. Acad. Sci. USA*. 99: 17203-17208.
8. Hayashi, F., H. Suzuki, R. Iwase, T. Uzumaki, A. Miyake, J. R. Shen, K. Imada, Y. Furukawa, K. Yonekura, K. Namba, and M. Ishiura. 2003. ATP-induced hexameric ring structure of the cyanobacterial circadian clock protein KaiC. *Genes to Cells*. 8:287-296.
9. Williams, S. B., I. Vakonakis, S. S. Golden, and A. C. LiWang. 2002. Structure and function from the circadian clock protein KaiA of *Synechococcus elongatus*: A potential

clock input mechanism. *Proc. Natl. Acad. Sci. USA.* 99:15357-15362.

10. Vakonakis, I., J. Sun, T. Wu, A. Holzenburg, S. S. Golden, and A. C. LiWang. 2004. NMR structure of the KaiC-interacting C-terminal domain of KaiA, a circadian clock protein: Implications for KaiA–KaiC interaction. *Proc. Natl. Acad. Sci. USA.* 101:1479-1484.

11. Garces, R. G., N. Wu, W. Gillon, and E. F. Pai. 2004. Anabaena circadian clock proteins KaiA and KaiB reveal a potential common binding site to their partner KaiC. *EMBO J.* 23:1688-1698.

12. Vakonakis, I., and A. C. LiWang. 2004. Structure of the C-terminal domain of the clock protein KaiA in complex with a KaiC-derived peptide: Implications for KaiC regulation. *Proc. Natl. Acad. Sci. USA.* 101:10925-10930.

13. Xu, Y., T. Mori, and C. H. Johnson. 2003. Cyanobacterial circadian clockwork: roles of KaiA, KaiB and the kaiBC promoter in regulating KaiC. *EMBO J.* 22: 2117-2126.

14. Ye, S., I. Vakonakis, T. R. Ioerger, A. C. LiWang, and J. C. Sacchettini. 2004. Crystal structure of circadian clock protein KaiA from *Synechococcus elongatus*. *J. Biol. Chem.* 279: 20511-20518.

15. Uzumaki, T., M. Fujita, T. Nakatsu, F. Hayashi, H. Shibata, N. Itoh, H. Kato, and M. Ishiura. 2004. Crystal structure of the C-terminal clock-oscillator domain of the cyanobacterial KaiA protein. *Nat. Struct. Mol. Biol.* 11: 623-631.

16. Pattanayek, R., D. R. Williams, S. Pattanayek, Y. Xu, T. Mori, C. H. Johnson, P. L. Stewart, and M. Egli. 2006. Analysis of KaiA-KaiC protein interactions in the cyano-bacterial circadian clock using hybrid structural methods. *EMBO J.* 25:2017-2028.

17. Iwase, R., K. Imada, F. Hayashi, T. Uzumaki, M. Morishita, K. Onai, Y. Furukawa, K. Namba, and M. Ishiura. 2005. Functionally important substructures of circadian clock protein KaiB in a unique tetramer complex. *J. Biol. Chem.* 280:43141-43149.

18. Hitomi, K., T. Oyama, S. Han, A. S. Arvai, and E. D. Getzoff. 2005. Tetrameric architecture of the circadian clock protein KaiB. A novel interface for intermolecular

interactions and its impact on the circadian rhythm. *J. Biol. Chem.* 280:19127-19135.

19. Tomita, J., M. Nakajima, T. Kondo, and H. Iwasaki. 2005. No Transcription—Translation Feedback in Circadian Rhythm of KaiC Phosphorylation. *Science*. 307:251-254.

20. Nakajima, M., K. Imai, H. Ito, T. Nishiwaki, Y. Murayama, H. Iwasaki, T. Oyama, and T. Kondo. 2005. Reconstitution of Circadian Oscillation of Cyanobacterial KaiC Phosphorylation in Vitro. *Science*. 308:414-415.

21. Kageyama, H., T. Nishiwaki, M. Nakajima, H. Iwasaki, T. Oyama, and T. Kondo. 2006. Cyanobacterial Circadian Pacemaker: Kai Protein Complex Dynamics in the KaiC Phosphorylation Cycle In Vitro. *Molecular Cell*. 23:161-171.

22. Terauchi, K., Y. Kitayama, T. Nishiwaki, K. Miwa, Y. Murayama, T. Oyama, and T. Kondo. 2007. ATPase activity of KaiC determines the basic timing for circadian clock of cyanobacteria. *Proc. Natl. Acad. Sci. USA*. 104:16377-16381.

23. Taeko, N., Y. Satomi, Y. Kitayama, K. Terauchi, R. Kiyohara, T. Takao, and T. Kondo. 2007. A sequential program of dual phosphorylation of KaiC as a basis for circadian rhythm in cyanobacteria. *EMBO J.* 26: 4029-4037.

24. Hiroshi, I., H. Kageyama, M. Mutsuda, M. Nakajima, T. Oyama, and T. Kondo. 2007. Autonomous synchronization of the circadian KaiC phosphorylation rhythm. *Nat. Struct. Mol. Biol.* 14:1084-1088.

25. Rust, M. J., J. S. Markson, W. S. Lane, D. S. Fisher, and E. K. O'Shea. 2007. Ordered Phosphorylation Governs Oscillation of a Three-Protein Circadian Clock. *Science*. 318:809-812.

26. Mori, T., D. R. Williams, M. O. Byrne, X. Qin, M. Egli, H. S. Mchaourab, P. L. Stewart, and C. H. Johnson. 2007. Elucidating the Ticking of an In Vitro Circadian Clockwork. *PLoS Biol.* 5:841-853.

27. van Zon, J. S., D. K. Lubensky, P. R. H. Altena, and P. R. ten Wolde. 2007. An allosteric model of circadian KaiC phosphorylation. *Proc. Natl. Acad. Sci. USA*.

104:7420-7425.

28. Yoda, M., K. Eguchi, T. P. Terada, and M. Sasai 2007. Monomer-Shuffling and Allosteric Transition in KaiC Circadian Oscillation. PLoS ONE. 2:e408.
29. Mehra, A., C. Hong, M. Shi, J. J. Loros, and J. C. Dunlap, Ruoff P. 2006. Circadian rhythmicity by autocatalysis. PLoS Comput. Biol. 2:e96.
30. Clodong, S., U. Düring, L. Kronk, A. Wilde, I. Axmann, H. Herzel, and M. Kollmann. 2007. Functioning and robustness of a bacterial circadian clock. Mol. Syst. Biol. 3:1-9.
31. Emberly, E., and N. S. Wingreen. 2006. Hourglass Model for a Protein-Based Circadian Oscillator. Phys. Rev. Lett. 96:038303.
32. Takigawa-Imamura, H., and A. Mochizuki. Predicting Regulation of the Phosphorylation Cycle of KaiC Clock Protein Using Mathematical Analysis. J. Biol. Rhythms. 21:405-416.
33. Gillespie, D.T. 1977. Exact stochastic simulation of coupled chemical reactions. J. Phys. Chem. 81:2340-2361.
34. Amdaoud, M., M. Vallade, C. W. Schaber, I. Mihalcescu. 2007. Cyanobacterial clock, a stable phase oscillator with negligible intercellular coupling. Proc. Natl. Acad. Sci. USA. 104:7051-7056.
35. Mihalcescu, I., W. Hsing, S. Leibler. Resilient circadian oscillator revealed in individual cyanobacteria. Nature. 2004. 430:81-5.

Supplementary Table

Reaction type	Reaction scheme	Rate constants	Values as used in the simulation	Values in standard units	
Phosphorylation	$T_i A_2 \rightarrow T_{i+1} A_2$	k_p^T	$1.4 \times 10^{-2} [\Delta t^{-1}]$	$4.1 \times 10^{-4} [\text{sec}^{-1}]$	
	$T_i A_2 \tilde{B}_4 \rightarrow T_{i+1} A_2 \tilde{B}_4$				
	$T_i A_2 B_4 \rightarrow T_{i+1} A_2 B_4$				
	Phosphorylation	$R_i A_2 \rightarrow R_{i+1} A_2$	k_p^R	$6.0 \times 10^{-3} [\Delta t^{-1}]$	$1.75 \times 10^{-4} [\text{sec}^{-1}]$
		$R_i A_2 \tilde{B}_4 \rightarrow R_{i+1} A_2 \tilde{B}_4$			
		$R_i A_2 B_4 \rightarrow R_{i+1} A_2 B_4$			
Dephosphorylation	$T_i \rightarrow T_{i-1}$	k_{dp}^T	$4.0 \times 10^{-3} [\Delta t^{-1}]$	$1.2 \times 10^{-4} [\text{sec}^{-1}]$	
	$T_i \tilde{A}_2 \rightarrow T_{i-1} \tilde{A}_2$				
	$R_i \rightarrow R_{i-1}$	k_{dp}^R	$1.1 \times 10^{-2} [\Delta t^{-1}]$	$3.2 \times 10^{-4} [\text{sec}^{-1}]$	
	$R_i \tilde{A}_2 \rightarrow R_{i-1} \tilde{A}_2$				
	$R_i \tilde{B}_4 \rightarrow R_{i-1} \tilde{B}_4$				
	$R_i B_4 \rightarrow R_{i-1} B_4$				
Association	$T_i + A_2 \rightarrow T_i \tilde{A}_2$	$k_b^{T-\tilde{A}}$	$2.5 \times 10^{-3} [\Delta t^{-1}]$	$1.2 \times 10^6 [\text{M}^{-1} \text{sec}^{-1}]$	
	$T_i \tilde{A}_2 \rightarrow T_i A_2$	$k_b^{T\tilde{A}-A}$	$5.0 [\Delta t^{-1}]$	$1.5 \times 10^{-1} [\text{sec}^{-1}]$	
	$T_i A_2 + B_4 \rightarrow T_i A_2 \tilde{B}_4$	$k_b^{TA-\tilde{B}}$	$1.0 \times 10^{-1} [\Delta t^{-1}]$	$5.0 \times 10^7 [\text{M}^{-1} \text{sec}^{-1}]$	
	$T_i A_2 \tilde{B}_4 \rightarrow T_i A_2 B_4$	$k_b^{TA\tilde{B}-B}$	$2.5 \times 10^{-1} [\Delta t^{-1}]$	$7.3 \times 10^{-3} [\text{sec}^{-1}]$	
	$R_i + A_2 \rightarrow R_i \tilde{A}_2$	$k_b^{R-\tilde{A}}$	$2.5 \times 10^{-2} [\Delta t^{-1}]$	$1.2 \times 10^7 [\text{M}^{-1} \text{sec}^{-1}]$	
	$R_i \tilde{A}_2 \rightarrow R_i A_2$	$k_b^{R\tilde{A}-A}$	$2.5 [\Delta t^{-1}]$	$7.3 \times 10^{-2} [\text{sec}^{-1}]$	
	$R_i A_2 + B_4 \rightarrow R_i A_2 \tilde{B}_4$	$k_b^{RA-\tilde{B}}$	$1.0 \times 10^{-2} [\Delta t^{-1}]$	$5.0 \times 10^6 [\text{M}^{-1} \text{sec}^{-1}]$	
	$R_i A_2 \tilde{B}_4 \rightarrow R_i A_2 B_4$	$k_b^{RA\tilde{B}-B}$	$2.0 \times 10^{-1} [\Delta t^{-1}]$	$5.8 \times 10^{-3} [\text{sec}^{-1}]$	

Reaction type	Reaction scheme	Rate constants	Values as used in the simulation	Values in standard units
Association	$R_i + B_4 \rightarrow R_i \tilde{B}_4$	$k_b^{R\tilde{B}}$	$1.0 \times 10^{-1} [\Delta t^{-1}]$	$5.0 \times 10^7 [M^{-1} \text{sec}^{-1}]$
	$R_i \tilde{B}_4 \rightarrow R_i B_4$	$k_b^{R\tilde{B}-B}$	$8.0 \times 10^{-1} [\Delta t^{-1}]$	$2.3 \times 10^{-2} [\text{sec}^{-1}]$
	$T_6 + B_4 \rightarrow T_6 \tilde{B}_4$	$k_b^{T_6\tilde{B}}$	$5.0 \times 10^{-3} [\Delta t^{-1}]$	$2.5 \times 10^6 [M^{-1} \text{sec}^{-1}]$
	$T_6 \tilde{A}_2 + B_4 \rightarrow T_6 \tilde{A}_2 \tilde{B}_4$	$k_b^{T_6\tilde{A}\tilde{B}}$	$5.0 \times 10^{-3} [\Delta t^{-1}]$	$2.5 \times 10^6 [M^{-1} \text{sec}^{-1}]$
	$2B_2 \rightarrow B_4$	$k_b^{2B_2-B_4}$	$2.0 \times 10^{-5} [\Delta t^{-1}]$	$1.0 \times 10^4 [M^{-1} \text{sec}^{-1}]$
Dissociation	$T_i \tilde{A}_2 \rightarrow T_i + A_2$	$k_d^{T\tilde{A}}$	$3.0 [\Delta t^{-1}]$	$8.7 \times 10^{-2} [\text{sec}^{-1}]$
	$T_i A_2 \rightarrow T_i + A_2$ $T_i A_2 \tilde{B}_4 \rightarrow T_i + A_2 + B_4$	k_d^{TA}	$5.0 [\Delta t^{-1}]$	$1.5 \times 10^{-1} [\text{sec}^{-1}]$
	$T_i A_2 \tilde{B}_4 \rightarrow T_i A_2 + B_4$	$k_d^{T\tilde{B}}$	$1.0 \times 10^{-1} [\Delta t^{-1}]$	$2.9 \times 10^{-3} [\text{sec}^{-1}]$
	$T_i A_2 B_4 \rightarrow T_i A_2 + B_4$	k_d^{TB}	$4.0 [\Delta t^{-1}]$	$1.2 \times 10^{-1} [\text{sec}^{-1}]$
	$R_i \tilde{A}_2 \rightarrow R_i + A_2$	$k_d^{R\tilde{A}}$	$2.0 \times 10^{-1} [\Delta t^{-1}]$	$5.8 \times 10^{-3} [\text{sec}^{-1}]$
	$R_i A_2 \rightarrow R_i + A_2$ $R_i A_2 \tilde{B}_4 \rightarrow R_i + A_2 + B_4$	k_d^{RA}	$9.0 \times 10^{-1} [\Delta t^{-1}]$	$2.6 \times 10^{-2} [\text{sec}^{-1}]$
	$R_i A_2 \tilde{B}_4 \rightarrow R_i A_2 + B_4$	$k_d^{R\tilde{B}}$	$1.0 \times 10^{-1} [\Delta t^{-1}]$	$2.9 \times 10^{-3} [\text{sec}^{-1}]$
	$R_i A_2 B_4 \rightarrow R_i A_2 + B_4$	k_d^{RB}	$2.5 [\Delta t^{-1}]$	$7.3 \times 10^{-2} [\text{sec}^{-1}]$
	$R_i \tilde{B}_4 \rightarrow R_i + B_4$	$k_d^{R\tilde{B}}$	$4.0 \times 10^{-1} [\Delta t^{-1}]$	$1.2 \times 10^{-2} [\text{sec}^{-1}]$
	$R_i B_4 \rightarrow R_i + B_4$	k_d^{RB}	$1.8 [\Delta t^{-1}]$	$5.2 \times 10^{-2} [\text{sec}^{-1}]$

Reaction type	Reaction scheme	Rate constants	Values as used in the simulation	Values in standard units
Dissociation	$T_6 \tilde{B}_4 \rightarrow T_6 + B_4$	$k_d^{T_6 \tilde{B}}$	$1.0 [\Delta t^{-1}]$	$2.9 \times 10^{-2} [\text{sec}^{-1}]$
	$T_6 \tilde{A}_2 \tilde{B}_4 \rightarrow T_6 \tilde{A}_2 + B_4$	$k_d^{T_6 \tilde{B}}$	$1.0 [\Delta t^{-1}]$	$2.9 \times 10^{-2} [\text{sec}^{-1}]$
	$R_6 B_4 \tilde{A}_2 \rightarrow R_6 B_4 + A_2$	$k_d^{R_6 \tilde{B}}$	$1.0 \times 10^{-1} [\Delta t^{-1}]$	$2.9 \times 10^{-3} [\text{sec}^{-1}]$
	$B_4 \rightarrow 2B_2$	$k_d^{B_4}$	$1.0 \times 10^{-1} [\Delta t^{-1}]$	$2.9 \times 10^{-3} [\text{sec}^{-1}]$
Allosteric transition	$T_6 \tilde{B}_4 \rightarrow R_6 B_4$	$k_{T \rightarrow R}^{T_6 \tilde{B}}$	$5.0 \times 10^{-5} [\Delta t^{-1}]$	$1.5 \times 10^{-6} [\text{sec}^{-1}]$
	$T_6 \tilde{A}_2 \tilde{B}_4 \rightarrow R_6 B_4 \tilde{A}_2$	$k_{T \rightarrow R}^{T_6 \tilde{B}}$	$5.0 \times 10^{-5} [\Delta t^{-1}]$	$1.5 \times 10^{-6} [\text{sec}^{-1}]$
	$R_0 \rightarrow T_0$	$k_{R \rightarrow T}^{R_0}$	$6.0 \times 10^{-3} [\Delta t^{-1}]$	$1.75 \times 10^{-4} [\text{sec}^{-1}]$
	$T_0 \rightarrow R_0$	$k_{T \rightarrow R}^{T_0}$	$2.0 \times 10^{-3} [\Delta t^{-1}]$	$5.8 \times 10^{-5} [\text{sec}^{-1}]$
	$R_0 \tilde{A}_2 \rightarrow T_0 + A_2$	$k_{R \rightarrow T}^{R_0 \tilde{A}}$	$6.0 \times 10^{-3} [\Delta t^{-1}]$	$1.75 \times 10^{-4} [\text{sec}^{-1}]$
	$R_0 \tilde{B}_4 \rightarrow T_0 + B_4$	$k_{R \rightarrow T}^{R_0 \tilde{B}}$	$6.0 \times 10^{-3} [\Delta t^{-1}]$	$1.75 \times 10^{-4} [\text{sec}^{-1}]$
Shuffling	$R_i + R_j \rightarrow R_k + R_l$	k_s^{RR}	$1.0 \times 10^{-4} [\Delta t^{-1}]$	$5.0 \times 10^4 [\text{M}^{-1} \text{sec}^{-1}]$
	$R_6 + T_i \rightarrow R_k + R_l$	k_s^{RT}	$2.0 \times 10^{-5} [\Delta t^{-1}]$	$1.0 \times 10^4 [\text{M}^{-1} \text{sec}^{-1}]$